Crystal Structure of CaiB, a Type-III CoA Transferase in Carnitine Metabolism†

Pål Stenmark, Daniel Gurmu, and Pär Nordlund*

Department of Biochemistry and Biophysics, Stockholm University, Roslagstullsbacken 15, Albanova University Center, SE-10691 Stockholm, Sweden

Received July 16, 2004; Revised Manuscript Received August 26, 2004

ABSTRACT: Carnitine is an important molecule in human metabolism, mainly because of its role in the transport of long-chain fatty acids across the inner mitochondrial membrane. *Escherichia coli* uses carnitine as a terminal electron acceptor during anaerobic metabolism. Bacteria present in our large intestine break down carnitine that is not absorbed in the small intestine. One part of this catabolic pathway is reversible and can be utilized for bioproduction of large amounts of stereochemically pure L-carnitine, which is used medically for the treatment of a variety of human diseases. Here, we present the crystal structure of the *E. coli* protein CaiB, which is a member of the recently identified type-III coenzyme A (CoA) transferase family and catalyzes the transfer of the CoA moiety between γ-butyrobetaine−CoA and carnitine forming carnityl-CoA and γ-butyrobetaine. This is the first protein from the carnitine metabolic pathway to be structurally characterized. The structure of CaiB reveals a spectacular fold where two monomers are interlaced to form an interlocked dimer. A molecule of the crystallization buffer bis-(2-hydroxyethyl)-imino-tris(hydroxymethyl)methane (bis-tris) is bound in a large pocket located primarily in the small domain, and we propose that this pocket constitutes the binding site for both substrate moieties participating in the CaiB transfer reaction. The binding of CoA to CaiB induces a domain movement that closes the active site of the protein. This is the first observation of a domain movement in the type-III CoA transferase family and can play an important role in coupling substrate binding to initiation of the catalytic reaction.

Carnitine plays several roles in human metabolism, with the most important being the transport of long-chain fatty acids across the inner mitochondrial membrane. Humans are able to synthesize carnitine, but the main source of this compound is from digesting meat and dairy products (*1*). Mammals are unable to metabolize carnitine except through microorganisms in the large intestine, which break down carnitine not taken up in the small intestine. There are two microbial catabolic pathways for carnitine present in the gut, one of which leads to the production of trimethylamine, which is mainly excreted through urine, while the other leads to the formation of γ-butyrobetaine, which is excreted through feces (*1*). We have solved the structure of CaiB from *Escherichia coli*, which is a coenzyme A (CoA)[1] transferase in the pathway leading to the formation of γ-butyrobetaine (*2*, *3*).

Some bacteria, including the genera *Pseudomonas*, are able to use carnitine as their sole carbon, nitrogen, and energy source. Bacteria from the genera *Acinetobacter* degrade the carnitine carbon backbone and form trimethylamine as a byproduct. CaiB, in the present study, is part of a third path for carnitine catabolism performed by members of the bacterial family Enterobacteriaceae such as *E. coli*. In this pathway, carnitine is converted via crotonobetaine to γ-butyrobetaine. In this way, carnitine is used as a terminal electron acceptor during anaerobic conditions, but growth requires additional carbon and nitrogen sources because the carbons and nitrogens from carnitine are not assimilated (*4*). Activity of this metabolic pathway has also been reported under aerobic conditions (*5*). Scheme 1 shows the reaction scheme for carnitine metabolism in *E. coli*, where **1**, carnitine; **2**, γ-butyrobetaine−CoA; **3**, γ-butyrobetaine; **4**, carnityl-CoA; and **5**, crotonobetainyl-CoA. There are three proteins directly involved in the conversion of carnitine to γ-butyrobetaine in *E. coli*: CaiA, CaiB, and CaiD. CaiD is a carnityl-CoA dehydratase, while CaiA is a crotonobetainyl-CoA reductase. Both enzymes act on CoA−thiosesters (*2*, *3*). CaiB is a CoA transferase that is able to move the CoA

Scheme 1

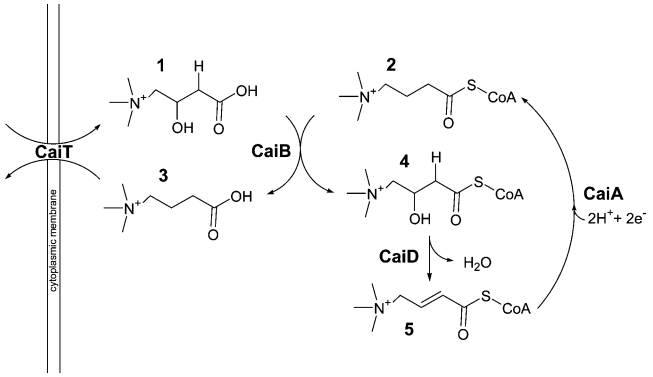

† This work was supported by the by the Swedish Research Council, the Wallenberg Consortium North, and the EU framework V Network SPINE.

* To whom correspondence should be addressed: Department of Biochemistry and Biophysics, Stockholm University, Roslagstullsbacken 15, Albanova University Center, SE-10691 Stockholm, Sweden. Phone: +46-8-55378587. Fax: +46-8-55378358. E-mail: par@dbb.su.se.

[1] Abbreviations: CoA, coenzyme A; FRC, formyl-CoA transferase; Se-Met, selenomethionine; IPTG, isopropyl-β-D-thiogalactopyransoside; HEPES, 4-(2-hydroxyethyl)-1-piperazineethanesulfonic acid; bis-tris (BTB), bis-(2-hydroxyethyl)imino-tris(hydroxymethyl)methane.

10.1021/bi048481c CCC: $27.50
Published on Web 10/09/2004

moiety from γ-butyrobetaine−CoA to carnitine, which forms carnityl-CoA and free γ-butyrobetaine. Carnityl-CoA is subsequently dehydrated by CaiD to form crotonobetainyl-CoA, which in turn is reduced by CaiA to form γ-butyrobetaine−CoA (Scheme 1) (*2*, *3*, *6*, *7*). It should be noted that the experimental evidence for this reaction scheme originates not from a complete reaction scheme but from two CaiB-dependent half reactions: (1) the hydratase reaction catalyzed by CaiD together with CaiB (*2*, *6*) and (2) the reductase reaction catalyzed by CaiA together with CaiB (*3*). In the first of the experimentally verified half reactions, CaiB catalyses the reversible exchange of the CoA moiety between the intermediate crotonobetainyl-CoA and carnitine (*2*). Because the dehydration reaction catalyzed by CaiD is also reversible it can, together with CaiB, be used industrially in bioproduction of large amounts of L-carnitine, using crotonobetaine as the starting material (*8*, *9*). This process produces L-carnitine in a stereochemically pure form, which is important when L-carnitine is used to treat a variety of human diseases (*10*). The *caiTABCDE* operon consists of six genes; a function has been suggested for most of these genes (*11*). CaiC is similar to a family of CoA ligases and most likely generates the initial carnityl-CoA needed for the CaiB reaction cycle, and it belongs to a family of CoA ligases that require ATP for the activation of the CoA molecule. CaiB does not require ATP to function; in fact, it would be a net loss of energy for the cell to use carnitine as a terminal electron acceptor if CaiC would be used to generate all of the carnityl-CoA instead of CaiB (*12*). The ATP-requiring CoA ligase (CaiC) is likely to be used only to generate enough carnityl-CoA to start the CaiB reaction cycle (*12*). CaiT has been shown to be a membrane-bound transporter responsible for the transport of the product γ-butyrobetaine out of the cell and the transport of the substrate carnitine into the cell (*13*). The function of the CaiE protein is unclear. The *caiTABCDE* operon is coregulated with the *fixABCX* operon (*14*, *15*). The *fixABCX* operon encodes proteins that are necessary for anaerobic carnitine reduction and are suggested to supply CaiA with the electrons necessary for the reduction of crotonobetainyl-CoA (*7*).

CaiB is a member of the recently discovered type-III CoA transferase family (*12*). The other two CoA transferase families have been well-characterized. The most widespread is the type-I family, this protein family catalyses CoA transfer using a ping-pong mechanism involving an enzyme-bound glutamyl-CoA−thioester. Type-II CoA transferases are much less common and have a mechanism involving a ternary complex (*12*). The first enzyme of the type-III CoA transferase family to be discovered was formyl-CoA transferase (FRC). FRC is involved in a reaction cycle where the CoA−thioester of oxalate is formed and then decarboxylated. The structure of FRC has recently been determined (*16*). The structure of an *E. coli* protein (YfdW) with high sequence similarity to FRC has also recently been solved. This protein is likely to be an *E. coli* FRC although this has not yet been demonstrated (*17*, *18*). The structures of FRC and YfdW reveal that the CoA sulfur moiety is positioned close to a conserved aspartic acid residue, which is proposed to serve as a catalytic nucleophile (*16*, *18*). FRC has also been studied in complex with the oxalyl-CoA product, revealing the formation of a covalent acylenzyme intermediate (*19*). The reaction kinetics of three different members of the type-III CoA transferase family have been studied; these data suggests that the reaction mechanism proceeds via a ternary complex in all proteins in this family (*19*−*21*). However, no detailed kinetic characterization of CaiB has yet been performed.

We describe here the high-resolution structure of CaiB solved using X-ray crystallography. The spectacular intertwined dimer fold previously seen in FRC and YfdW is also present in CaiB and is likely to be present in all members of the type-III CoA transferase family. We also show that CoA binding induces a domain movement that closes the active site. In contrast to FRC and YfdW, a large cavity is found in CaiB, which can harbor the larger ternary complex likely to be formed in CaiB and several other members of the type-III CoA transferases.

MATERIAL AND METHODS

Protein Production. The *E. coli caiB* gene was subcloned into the *E. coli* expression vector PT73.3 (*22*) using the Gateway system (Invitrogen, Carlsbad, CA). The resulting vector encoded a polypeptide with the *caiB* gene that has an N-terminal add on (N-MHHHHHHGSTSLYKKAGSETLYIQG-), which encompasses an attB site for the Gateway recombination event and a hexahistidine sequence to simplify purification. An additional C-terminal hexahistidine tail (-STHHHHHH-C) was used to monitor full-length protein production. The *caiB* gene was overexpressed in BL21(DE3) cells in M9 minimal salts (MM) to facilitate the incorporation of selenomethionine (Se-Met) into the protein using the methionine pathway inhibition method (*23*). The media contained 239 mM disodium phosphate, 110 mM monopotassium phosphate, 43 mM sodium chloride, 93 mM ammonium chloride, 22 mM glucose, 2 mM $MgSO_4$, 0.1 mM $CaCl_2$, 0.01 mM $MnCl_2$, 0.01 mM $FeSO_4$, and tetracycline (30 μg/mL). An overnight culture of 50 mL was prepared from which 10 mL per liter were used to inoculate a final volume of 5 L. The flasks were incubated in a shaker at 37 °C (200 rpm) until an OD_{600} of ∼0.6 was obtained. At that time, the temperature was dropped to 18 °C and an amino acid mixture (100 mg lysine, 100 mg threonine, and 100 mg phenylalanine together with 50 mg of leucine, 50 mg isoleucine, 50 mg valine, and 50 mg of L-Se-Met per liter) was added prior to induction with isopropyl-β-D-thiogalactopyransoside (IPTG) to a final concentration of 0.25 mM. The cells grew at 18 °C overnight and were harvested by centrifugation at 9000*g* for 15 min.

Protein Purification. The cells were disrupted using sonication in lysis buffer [20 mM sodium phosphate at pH 7.4, 0.5 M NaCl, 20 mM imidazole, 10 mM β-mercaptoethanol, 10% (v/v) glycerol, 0.08 mg/mL lysozyme, 0.4 mg/mL DNAse I, and Complete ethylenediaminetetraacetic acid (EDTA)-free Protease Inhibitor tablets (Roche Diagnostics GmbH, Mannheim, Germany)]. After sonication, the cells were centrifuged at 50000*g* for 20 min, and the supernatant was passed through a 0.22-μm filter, for the removal of cell debris, before being loaded on a Ni^{2+}-loaded Hi-Trap Chelating column (Amersham Biosciences, Uppsala, Sweden) pre-equilibrated in wash buffer (lysis buffer without lysozyme and DNAse I). The His-tagged CaiB protein was eluted with elution buffer (same as the wash buffer but with 200 mM imidazole). To obtain CaiB of crystallization-grade quality,

Table 1: Crystallographic Data for CaiB from *E. coli*

data statistics	CaiB	CoA complex
wavelength (Å)	0.980 (Se peak)	1.09
space group	$P2_1$	$P2_1$
cell dimensions (Å): a, b, c	55.6, 129.8, 69.8	55.6, 125.7, 70.0
cell angles (deg): α, β, γ	90.0, 109.5, 90.0	90.0, 109.0, 90.0
resolution (Å) (outer shell)	30−1.85 (1.95−1.85)	30−1.90 (2.00−1.90)
number of observations (unique)	288 389 (76 742)	278 901 (70 549)
R_{sym} (outer shell)[a]	0.092 (0.18)	0.067 (0.23)
$I/\sigma(I)$ (outer shell)	5.82 (3.46)	7.71 (3.01)
completeness (%) (outer shell)	96.8 (89.4)	98.9 (95.5)
redundancy (outer shell)	3.76 (3.42)	3.95 (3.70)
Refinement and Ramachandran Plot Statistics		
R_{cryst} (%)[b]	14.3	14.4
R_{free} (%)[c]	17.8	17.6
non-H atoms	6933	6911
solvent molecules	644	588
rms deviation bonds (Å)	0.018	0.018
rms deviation angles (deg)	1.485	1.459
average *B* factors (Å^2)		
protein	19.4	20.8
bis-tris	24.4	35.3
CoA		44.0
Ramachandran plot		
core	92	91.9
allowed	7.4	7.5
generously allowed	0.4	0.4
disallowed	0.1	0.1

[a] $R_{sym} = \sum_j\sum_h|\langle I_{hj} - I_h\rangle|/\sum_j\sum_h I_{jh}$, where I_{hj} is the jth observation of reflection h. [b] $R_{cryst} = \sum||F_{obs} - F_{calc}||/|\sum_{obs}|$, where F_{obs} and F_{calc} are the observed and calculated structure factor amplitudes, respectively. [c] R_{free} is equivalent to R_{cryst} for a 5% subset of reflections not used in the refinement.

a second purification step was used. The fractions containing the protein of interest from the Ni-affinity chromatography were pooled and subjected to a HiLoad 26/60 Superdex 200 gel-filtration column (Amersham Biosciences), pre-equilibrated in gel-filtration buffer [20 mM 4-(2-hydroxyethyl)-1-piperazineethanesulfonic acid (HEPES) at pH 7.4, 150 mM NaCl, 10 mM β-mercaptoethanol, 10% (v/v) glycerol, and 2 mM EDTA]. The eluted fractions from the gel-filtration column, which contained the CaiB protein, were pooled and concentrated to a final volume of 40 mg/mL using an Amicon Ultra centrifugal filter device (Millipore, Bedford, MA). The protein concentration was estimated by UV absorption based on a calculated absorption molar coefficient of 61 950 M^{-1} cm^{-1} at 280 nm.

Protein Crystallization and Structure Determination. Initial crystallization trials were performed at a protein concentration of 11 mg/mL, using the sitting-drop vapor-diffusion method and sparse-matrix screens Crystal Screen, Crystal Screen 2, and Index (Hampton Research, CA) in 96-well plates from Intelli-plate (Art Robbins Enterprises, Mountain View, CA) at two different temperatures, 20 and 7 °C. Drops containing 0.9 μL of protein solution were mixed with 0.9 μL of crystallization solution and equilibrated against a reservoir solution containing a larger volume (100 μL) of well solution. Initial crystals were obtained in multiple conditions. Solution number 66 from Index produced one of the initial hits. Further optimizations around this condition were carried out using the hanging-drop vapor-diffusion method. Good-quality crystals of the Se-Met-labeled protein were obtained in 0.2 M ammonium sulfate, 0.1 M bis-(2-hydroxyethyl)imino-tris(hydroxymethyl)methane (bis-tris) at pH 5.2−6.1, and 20−23% (w/v) poly(ethylene glycol) 3350 at 20 °C. The crystals were cryo-protected in 20% (v/v) glycerol and mother liquor before being flash-frozen in liquid nitrogen. CaiB crystallized in the space group $P2_1$ and diffracted to beyond 1.85 Å resolution. A single-wavelength anomalous dispersion data set at the Se peak was collected at beam-line PSF-BL1 (BESSY, Berlin, Germany). The data were processed and scaled using DENZO and SCALEPACK (*24*), and SOLVE (*25*) was able to identify 30 of the 34 selenium sites present in the asymmetric unit. After density modification using RESOLVE (*26*), which produced very nice maps, ARP/wARP (*27*) was used to build ~95% of the structure. The data were reprocessed using MOSFLM (*28*) (Table 1), and the final models were obtained after multiple rounds of rebuilding and refinement using O (*29*) and REFMAC5 (*30*). Automated water building was carried out using the ARP/wARP program package. The free *R* value was calculated from 5% of the data and monitored throughout the refinement. CaiB was also crystallized in the presence of ~7 mM CoA, using the same crystallization conditions as for the apo structure. Streak-seeding was necessary to obtain crystals, which also belonged to the spacegroup $P2_1$ and diffracted to 1.9 Å. The data for the CoA complex was collected at the Max-Lab I711 beam line in Lund, Sweden. These data were processed using MOSFLM (*28*) (Table 1), and phases were obtained by molecular replacement with MOLREP (*31*) using the apo structure as the template. Otherwise, the CoA complex was refined in the same way as the apo structure. It was possible to trace the proteins from amino acid 4 to 403 of 405, and both of the final models have good *R* values and stereochemistry (Table 1). Asp 76 from chain A in the dimer and Glu 23 from both chains fall in the generously allowed region of the Ramachandran plot. Both of these residues are located in loop regions and are clearly defined in the electron density. Asp 76 from the chain B of the dimer falls in the disallowed region of the Ramachandran plot; this residue is also located in a loop region, and it makes a crystal contact that distorts it somewhat. Asp 76 from chain B is clearly defined in the

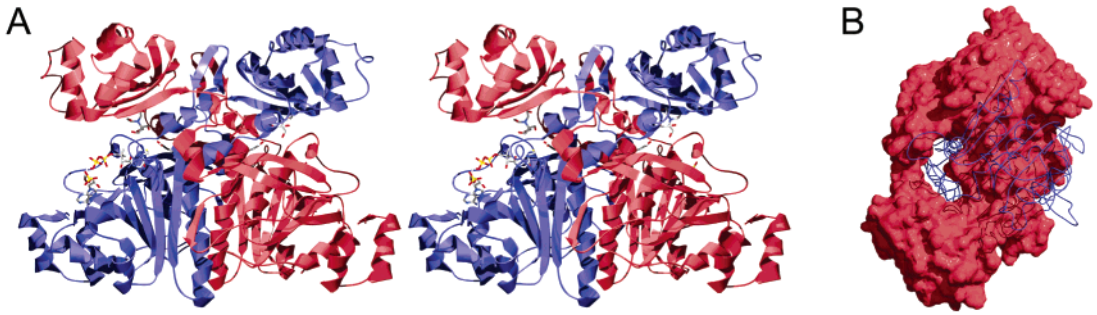

FIGURE 1: (A) Ribbon representation of the CaiB dimer in stereo. One chain is colored red, and the other is colored blue. CoA, bis-tris, and the catalytically important Asp 169 are shown in a stick representation. (B) CaiB dimer. One protein chain of the dimer is shown as a spacefill in red, and the other chain is shown as a blue thread. This illustrates the fold with the monomers interlaced to form an interlocked dimer.

electron density. Two cis prolines are present in the structures, Pro 165 and Pro 358. The protein−protein interaction server (http://www.biochem.ucl.ac.uk/bsm/PP/server/) was used to analyze the dimer interface. Pictures were produced using Swiss-PdbViewer (*32*), POV-ray (Persistence of Vision Development Team), and LIGPLOT (*33*). Coordinates and structure factors have been deposited in the Protein Data Bank (PDB). The ID code for the CaiB structure is 1XA3 and 1XA4 for the CoA complex.

RESULTS AND DISCUSSION

We have solved the crystal structure of CaiB from *E. coli* and its complex with CoA. The structure of CaiB reveals a dimer in the asymmetric unit. The dimer has an unusual fold where the two monomers are folded around each other, like interlaced rings (Figure 1). Each 405 amino acid monomer could be traced from amino acid 4 to 403 and encompass one small domain and one large domain. The active site of CaiB is located in a crevice between the large domain of one monomer and the small domain of the other monomer (Figure 1). The large domain of CaiB consists of both the N-terminal part of the protein (residues 4−208) and the C-terminal part of the protein (residues 338−403), and the small domain is located between (residues 227−323). The structure of the large domain of CaiB is very similar to the structure of the large domain of FRC (Figure 2A) (*16*), which was expected, based on the approximately 30% sequence identity in the region of the large domain. The small domain of CaiB displays no significant sequence identity to FRC, and it was therefore unclear whether this part of CaiB would have the same fold as the small domain of FRC. The structure of the small domain of CaiB is quite different from the FRC counterpart, but it is clear that they have evolved from the same origin based on their similar topology. Figure 2 shows the CaiB structure superimposed on the FRC structure. The largest difference between the CaiB and the FRC structures is in a 36 amino acid loop following helix 11 in FRC and preceding the start of the small domain, which in CaiB is 20 amino acids shorter than in FRC. The absence of this loop in CaiB leads to the removal of a glycine-rich loop that points directly into the active site of FRC (Figure 2b), which creates a large pocket in the active-site region of CaiB. The loop was observed to adopt different conformations in FRC depending on CoA binding and has been suggested to have a role in catalysis (*16*). The larger active-site pocket in CaiB seems logical because carnitine is twice the size of oxalate. This loop is also missing a number of other enzymes in this

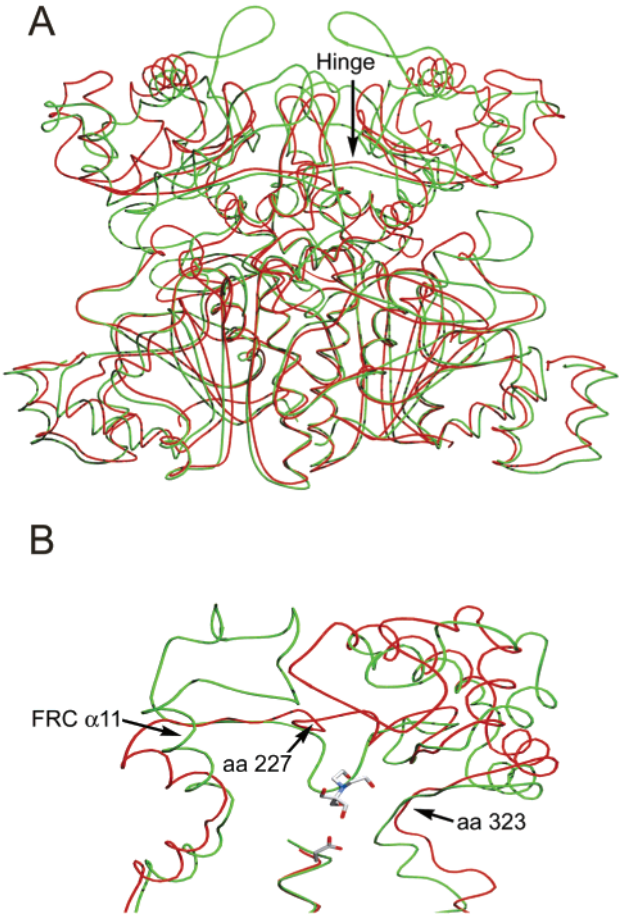

FIGURE 2: (A) Apo structure of CaiB superimposed on the FRC apo structure [PDB ID 1P5H (*16*)]. CaiB is shown in red, and FRC is shown in green. The hinge region is more pronounced in the CaiB structure. (B) Close up of the superimposed structures, showing only the small domain from one chain and the neighboring loop regions. The bis-tris molecule and Asp 169 from CaiB are shown in a stick representation. A portion of the helices containing Asp 169 is also displayed. The glycine-rich loop from FRC is situated on top of the bis-tris molecule from CaiB. The hinge is located at the start (amino acid 227) and end (amino acid 323) of the small domain.

family, specifically those that bind larger substrates than FRC. The shorter loop also leads to a more pronounced hinge region between the large and small domains of CaiB, which is located at the start (amino acid 227) and end (amino acid 323) of the small domain.

Bis-tris Binding in the Active Site. During refinement of both the apo and the CoA complex structures, a large body

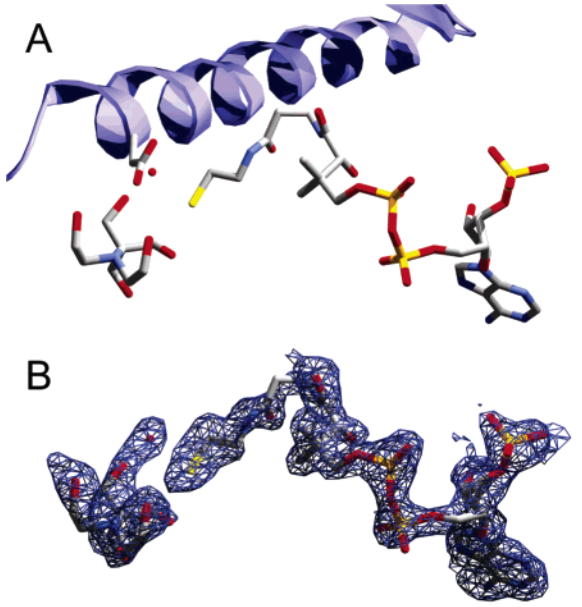

FIGURE 3: Active site of CaiB. (A) Asp 169 is shown in a stick representation, and the backbone helix is shown as a ribbon. The bis-tris molecule and the CoA molecule are shown in a stick representation, and a water present in the active site is also shown. The rest of the protein has been omitted. (B) Simulated annealing omit map of the CoA molecule, the bis-tris molecule, and water. The molecules are orientated in the same way as in A.

of electron density was found in the active site. Bis-tris, the buffer used for crystallization, fit this electron density very well (Figure 3B). The bis-tris molecule is bound in a large cavity in the active site that most likely constitutes the substrate-binding pocket. The bis-tris molecule is highly polar, as are the substrates, but do not have the zwitterionic features of the carnitine-like substrate moieties (although the nitrogen of bis-tris might become positively charged in acidic environments). Bis-tris is also a significantly bulkier molecule than a single carnitine-like moiety of the substrate, and our hypothesis is that the pocket where the bis-tris molecule binds might in fact constitute the binding site for both of the carnitine-like moieties that are involved in the transfer reaction. Glu 249 and Glu 23 are located on two different walls of the pocket in suitable positions to compensate for the positive charge on the nitrogen of the crotonobetaine, γ-butyrobetaine, or carnitine molecule (Figure 4A). Glu 23 also falls in the generously allowed region of the Ramachandran plot but is clearly defined by the electron density. Such strained geometry is often indicative of an important function of the residue. Other residues are also well-positioned to contribute with hydrophobic interactions and hydrogen bonds to the substrate (Figure 4A). The bis-tris molecule also makes a hydrogen bond to the catalytically important and completely conserved Asp 169 (Figure 4A). This aspartic acid also makes a hydrogen bond to the SH group of CoA in the CoA complex structure (Figure 4B). Soaking, cocrystallization, and rescreening trials with carnitine have failed to displace the bis-tris molecule. When superimposing the FRC structure with the CaiB structure, the bis-tris molecule is located in the same position as the flexible glycine-rich loop from FRC. This loop is absent in CaiB and the bis-tris molecule fills the void. When the glycine-rich loop from FRC is in its open position, the overlap with the bis-tris molecule is smaller but the active-site pocket is still considerably larger

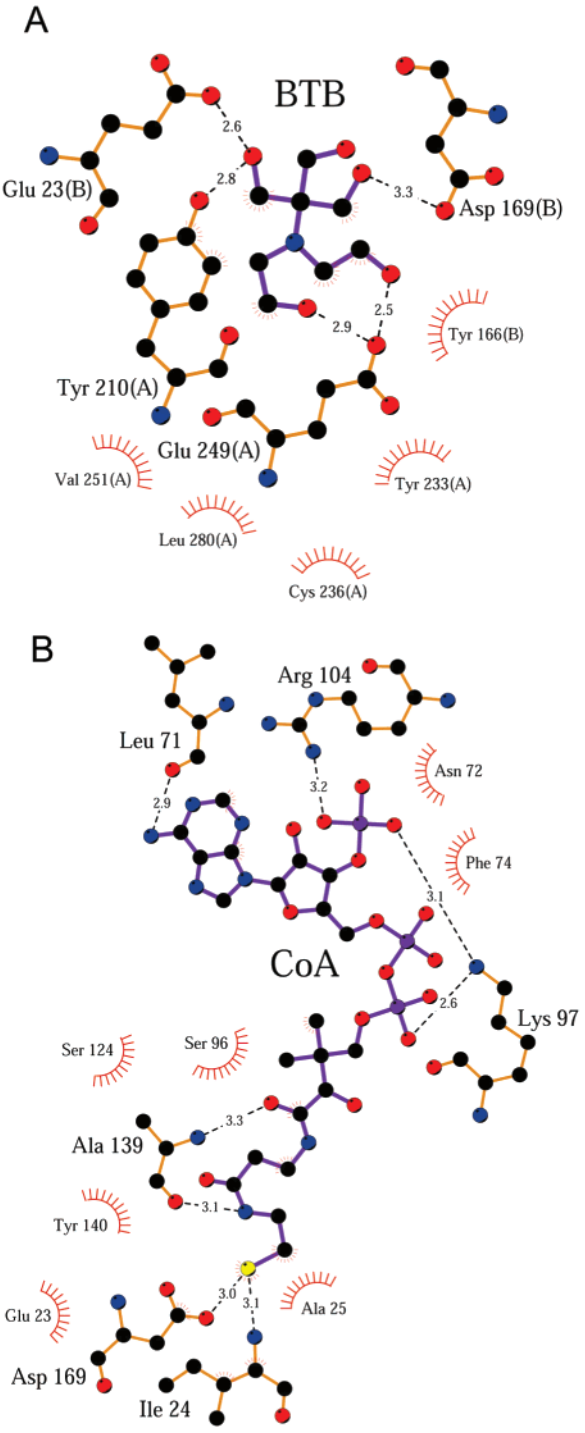

FIGURE 4: Schematic representation of the ligand interactions with CaiB. Hydrogen bonds are indicated with dotted lines, and the hydrogen-bond distances are shown. Residues involved in hydrophobic interactions with the ligand are shown with red rays. (A) Interactions between bis-tris (BTB) and the protein. Both the A and B chains are interacting with bis-tris. (B) Interactions between CoA and CaiB. All residues interacting with the CoA molecule are originating from the B chain.

in the CaiB structure. The small domain makes up the majority of the substrate-binding pocket, and this domain also makes most of the contacts with the bis-tris molecule (Figure 4A). Multiple sequence alignments between proteins from the type-III CoA transferase family show that the large domain is reasonably well-conserved, while the small domain shows a very low degree of conservation (*12*, *16*). On the basis of the structure of the substrate-binding pocket of CaiB,

a high degree of variability in the small domain would be necessary to adapt to the variety of substrates used by the type-III CoA transferases.

Type-III CoA Transferase Fold. Despite the very low sequence identity between the small domains of CaiB and FRC (*12*, *16*), both of these CoA transferases are folded as interlocked dimers. It is very likely that most other members of the type-III CoA transferase family have this intriguing fold. It is unlikely that monomeric proteins of this fold exist. We therefore propose that all members of the type-III CoA transferase family are dimeric or consist of several dimeric units. The folding of CaiB and other proteins of this fold must be quite complex because the dimer cannot be formed by the individually folded monomers. Multiple ribosomes are often present on the same mRNA, which opens for the possibility that partially synthesized peptide chains coming from two different ribosomes located on the same mRNA might cofold before translation is finished. Another possibility is that the monomers are able to exist as unfolded structures in solution before dimerization induces the final folding of the individual monomers (*16*). There is an area in the large domain that contains a number of residues that are highly conserved in the type-III CoA transferase family (CaiB numbering: Arg 16, Gly 37, Ala 38, Val 40, Asp 90, Leu 184, His 185, Gly 193, and Thr 190). These residues may be important for folding. The unusual fold of CaiB creates a very large dimer interface (~6100 Å^2), with 150 of the 405 amino acids making interactions across the dimer interface. The partial unfolding that would have to take place to break apart the CaiB dimer and the extensive interactions across the dimer interface could be expected to lead to a very stable dimer. The thermally induced melting point of CaiB is 42 °C, which is surprisingly low (Stenmark unpublished). The melting point was obtained using a fluorescence-based thermal shift assay (*34*).

Binding of CoA Induces a Domain Movement. One dimer of CaiB is present in the asymmetric unit, and each monomer has one potential CoA-binding site. Because of the crystal packing, only one of the two CoA-binding sites are occupied. A large crevice is present between the small and large domains, but these two domains originate from different monomers in the structure. The CoA molecule binds to the side of the crevice but makes interactions only to the large domain. Because the CoA binding is common to all of the members of the transferase family, it is logical that the large domain, which is responsible for the interactions with CoA, is much more conserved through the protein family than the small, substrate-binding domain. The positively charged amino acids Lys 97 and Arg 104 coordinate the phosphate groups of the CoA molecule (Figure 4B). A lysine and two arginines coordinate the CoA molecule in the FRC structure (*16*). The lysines are located in similar positions in space in the CaiB and FRC structures, but they originate from different parts of the polypeptides. Ala 139 of CaiB makes two hydrogen bonds to the pantetheine chain of the CoA molecule; these two hydrogen bonds induce a rotation of the residue that is not present in the apo structure. Many hydrophobic interactions also contribute to the binding of the CoA molecule (Figure 4B). The SH group makes one hydrogen bond to the main-chain amino group of Ile 24 and one to the carboxyl group of Asp 169, which has been proposed to carry a covalent intermediate in the reaction

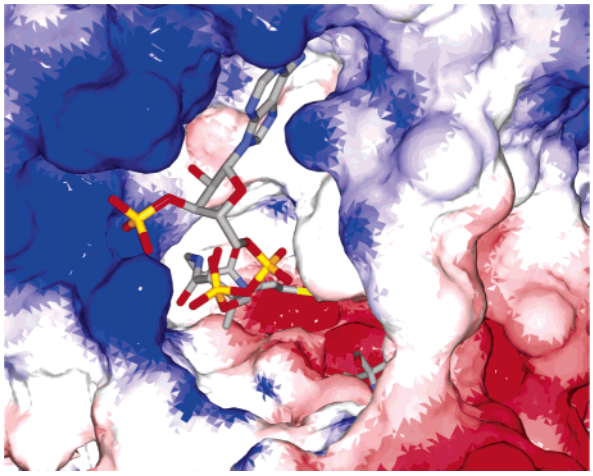

FIGURE 5: Molecular structure of the CaiB active site. The CoA and the bis-tris molecules are shown in a stick representation. Bis-tris is only partly visible deep inside the active-site pocket.

mechanisms of this protein family (*16*, *18*, *19*). The CoA-binding crevice and part of the bis-tris-binding pocket of CaiB are displayed in Figure 5. The main difference between the CoA binding of FRC and CaiB is a rearrangement of the pyrophosphate. Both the adenine and pantetheine part of the CoA molecule bind in a very similar position in the two structures, but interestingly, the interactions that position the CoA molecules are quite different. When no CoA is bound to the protein, Arg 104 coordinates a sulfate. When CoA is bound, this residue instead coordinates the phosphate group on the ribose of the CoA molecule. When CaiB binds CoA, the small domain moves closer to the large domain, which leads to a more closed active site. The hinge is located at the start (amino acid 227) and end (amino acid 323) of the small domain, and the movement is approximately 3 Å in the area furthest away from the hinge. It is possible that the domain movement will be even larger in the presence of the actual substrate instead of just the CoA moiety (and the bis-tris molecule). It has been reported that CaiB, in the presence of the substrate, associates with CaiA (the crotonobetainyl-CoA reductase) (*3*). Because this interaction is only seen in the presence of the substrate, it is possible that the domain movement that we have observed in CaiB could be responsible for the formation of this interaction. In the structural study of YfdW, the potential *E. coli* homologue of FRC, structural differences were also observed between the apo and CoA complex structures, but these changes are mainly located at the surface of the large domain (*18*). In two other studies of FRC and YfdW, no large structural differences were observed upon CoA binding (*16*, *17*). A more closed active site might be necessary to protect the activated $CoAS^-$ anion and/or the enzyme−anhydride intermediate during the reaction. Maybe the flexible glycine-rich loop present in the active site of FRC and the domain movement in CaiB are two different modes of obtaining this shielding effect. FRC is an outlier from the type-III CoA transferase family in respect to their small substrate size. FRC also has an insertion in the area of the CaiB hinge that probably makes this region more rigid (Figure 2). This insertion is absent from all other characterized members of the enzyme family, indicating that the domain movement identified in the CoA complex of CaiB might be a general feature of most type-III CoA transferase proteins.

Scheme 2

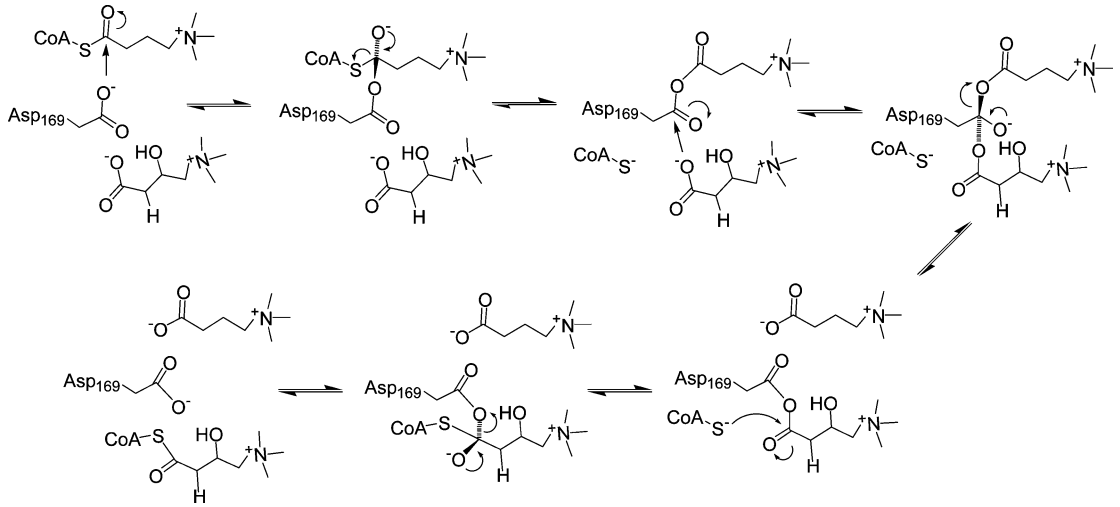

Reaction Mechanism of CaiB. A plausible reaction mechanism, based on kinetic and structural studies of FRC, has been suggested for the type-III CoA transferase family (*16*, *19*), involving covalent enzyme substrate intermediates. Strong evidence for the formation of such intermediates was recently provided by the structural characterization of an oxalyl-aspartyl anhydride in FRC (*19*). Several mutants of FRC have also been constructed, where the nucleophilic Asp 169 was mutated to alanine, serine, or glutamic acid (*19*). Both the D169S and D169E mutants were, as expected, completely inactive, but surprisingly, the D169A mutant retained a very low but detectable activity. A different but still unidentified reaction mechanism was suggested to account for this residual activity (*19*). These mutational studies show the importance of Asp 169 in FRC, and structural comparisons of CaiB with FRC suggest that Asp 169 play a similar role in both enzymes. If the suggested reaction mechanism is applied for CaiB, γ-butyrobetaine−CoA will react with Asp 169 to form an intermediate, where γ-butyrobetaine is bound covalently to Asp 169 and $CoAS^-$ is formed. Carnitine then reacts with the covalent intermediate to form a new intermediate, where carnitine is covalently bound to Asp 169. This part of the reaction will produce γ-butyrobetaine. The $CoAS^-$ anion now attacks the enzyme−anhydride intermediate, generating the product carnityl-CoA and regenerating the nonmodified Asp 169. Scheme 2 shows the proposed reaction mechanism for CaiB. The scheme is adapted from Jonsson et al. (*19*). The reaction has several negatively charged tetrahedral transition states. These have been suggested to be stabilized by Tyr 59 in the FRC structure (*16*); the corresponding residue, Tyr 58, in CaiB is located 8.5 Å from Asp 169. A quite large structural rearrangement would have to take place to put Tyr 58 in a suitable position for this stabilization. Gln 17 in FRC has also been suggested to stabilize the tetrahedral transition states (*19*). This residue is not conserved in the CaiB protein, and an isoleucine (Ile 24) is present in its place. This isoleucine is unable to provide such stabilization but is suitable for interactions with carnitine, which is a more hydrophobic substrate than oxalate. It is unlikely that either of the two suggested residues are uniformly involved in the stabilization of tetrahedral transition states in the reaction mechanism of type-III CoA transferase proteins. A common feature between these enzymes is the two main-chain NH (residues Ile 24 and Ala 25) interactions with the CoA sulfur anion, which can function to stabilize an anionic $CoAS^-$ intermediate. Kinetic studies for members of the type-III CoA transferase family suggest the existence of a ternary complex during substrate turnover. When we extrapolate to CaiB, this implies that the aspartic anhydride of γ-butyrobetaine would be present in the active site at the same time as carnitine, requiring significant space. Carnitine is a thinner molecule than the bis-tris that occupies our active site. Modeling indicates that the aspartic anhydride of γ-butyrobetaine can reside in the substrate-binding site at the same time as carnitine and CoA. A key feature for catalysis is then very likely the prepositioning of all of the groups involved in the transfer reactions in close proximity; therefore, group exchange can be performed with only small conformational realignment of the groups. There are however no additional obvious conserved features present in the active site, which can directly assist in bond formation or breakage steps or in the stabilization of intermediates in the reaction path.

In Summary. We have determined the structure of CaiB, a member of the recently discovered type-III CoA transferase family. This constitutes the first enzyme in carnitine metabolism that has been structurally characterized. The structure shows an intriguing fold with two interlaced monomers forming the protein dimer. This fold is very likely representative of the entire type-III CoA transferase family. We have described the relatively large substrate-binding pocket, which is probably common for most members of this enzyme family. In addition, we propose that the high degree of sequence variability in the small domain is necessary to adapt to the various substrates used by the different members of the type-III CoA transferase family. We have also shown that CoA binding induces a domain movement that closes the active site, possibly to protect reactive intermediates during catalysis. This is the first observation of a domain movement in the type-III CoA transferase family, and we believe that this may be a general feature for many members of this enzyme family.

ACKNOWLEDGMENT

We thank Yngve Cerenius for assistance at the I711 beam line at MAX-Lab (Lund, Sweden) and Uwe Müller and Martin Fieber-Erdmann at PSF-BESSY (Berlin, Germany)

for support at beam-line BL1. We also thank Ulrika Ericsson for help with the ÄKTA systems and the fluorescence-based thermal shift assay analysis. Benita Engvall is acknowledged for cloning the *caiB* gene. Albert Beuscher and Heidi Erlandsen are thanked for help with the manuscript.

REFERENCES

1. Rebouche, C. J., and Seim, H. (1998) Carnitine metabolism and its regulation in microorganisms and mammals, *Annu. Rev. Nutr. 18*, 39−61.
2. Elssner, T., Engemann, C., Baumgart, K., and Kleber, H. P. (2001) Involvement of coenzyme A esters and two new enzymes, an enoyl-CoA hydratase and a CoA-transferase, in the hydration of crotonobetaine to L-carnitine by *Escherichia coli*, *Biochemistry 40*, 11140−11148.
3. Preusser, A., Wagner, U., Elssner, T., and Kleber, H. P. (1999) Crotonobetaine reductase from *Escherichia coli* consists of two proteins, *Biochim. Biophys. Acta 1431*, 166−178.
4. Kleber, H. P. (1997) Bacterial carnitine metabolism, *FEMS Microbiol. Lett. 147*, 1−9.
5. Elssner, T., Preusser, A., Wagner, U., and Kleber, H. P. (1999) Metabolism of L(−)-carnitine by Enterobacteriaceae under aerobic conditions, *FEMS Microbiol. Lett. 174*, 295−301.
6. Elssner, T., Hennig, L., Frauendorf, H., Haferburg, D., and Kleber, H. P. (2000) Isolation, identification, and synthesis of γ-butyrobetainyl-CoA and crotonobetainyl-CoA, compounds involved in carnitine metabolism of *E. coli*, *Biochemistry 39*, 10761−10769.
7. Walt, A., and Kahn, M. L. (2002) The fixA and fixB genes are necessary for anaerobic carnitine reduction in *Escherichia coli*, *J. Bacteriol. 184*, 4044−4047.
8. Obon, J. M., Maiquez, J. R., Canovas, M., Kleber, H. P., and Iborra, J. L. (1999) High-density *Escherichia coli* cultures for continuous L(−)-carnitine production, *Appl. Microbiol. Biotechnol. 51*, 760−764.
9. Jung, H., Jung, K., and Kleber, H. P. (1993) Synthesis of L-carnitine by microorganisms and isolated enzymes, *Adv. Biochem. Eng. Biotechnol. 50*, 21−44.
10. Kerner, J., and Hoppel, C. (1998) Genetic disorders of carnitine metabolism and their nutritional management, *Annu. Rev. Nutr. 18*, 179−206.
11. Eichler, K., Bourgis, F., Buchet, A., Kleber, H. P., and Mandrand-berthelot, M. A. (1994) Molecular characterization of the cai operon necessary for carnitine metabolism in *Escherichia coli*, *Mol. Microbiol. 13*, 775−786.
12. Heider, J. (2001) A new family of CoA-transferases, *FEBS Lett. 509*, 345−349.
13. Jung, H., Buchholz, M., Clausen, J., Nietschke, M., Revermann, A., Schmid, R., and Jung, K. (2002) CaiT of *Escherichia coli*, a new transporter catalyzing L-carnitine/γ-butyrobetaine exchange, *J. Biol. Chem. 277*, 39251−39258.
14. Buchet, A., Eichler, K., and Mandrand-Berthelot, M. A. (1998) Regulation of the carnitine pathway in *Escherichia coli*: Investigation of the cai-fix divergent promoter region, *J. Bacteriol. 180*, 2599−2608.
15. Eichler, K., Buchet, A., Bourgis, F., Kleber, H. P., and Mandrand-berthelot, M. A. (1995) The Ffix *Escherichia coli* region contains 4 genes related to carnitine metabolism, *J. Basic Microbiol. 35*, 217−227.
16. Ricagno, S., Jonsson, S., Richards, N., and Lindqvist, Y. (2003) Formyl-CoA transferase encloses the CoA binding site at the interface of an interlocked dimer, *EMBO J. 22*, 3210−3219.
17. Gogos, A., Gorman, J., and Shapiro, L. (2004) Structure of *Escherichia coli* YfdW, a type III CoA transferase, *Acta Crystallogr., Sect. D 60*, 507−511.
18. Gruez, A., Roig-Zamboni, V., Valencia, C., Campanacci, V. R., and Cambillau, C. (2003) The crystal structure of the *Escherichia coli* YfdW gene product reveals a new fold of two interlaced rings identifying a wide family of CoA transferases, *J. Biol. Chem. 278*, 34582−34586.
19. Jonsson, S., Ricagno, S., Lindqvist, Y., and Richards, N. G. (2004) Kinetic and mechanistic characterization of the formyl-CoA transferase from *Oxalobacter formigenes*, *J. Biol. Chem. 279*, 36003−36012.
20. Leutwein, C., and Heider, J. (2001) Succinyl-CoA:(*R*)-benzylsuccinate CoA-transferase: An enzyme of the anaerobic toluene catabolic pathway in denitrifying bacteria, *J. Bacteriol. 183*, 4288−4295.
21. Dickert, S., Pierik, A. J., Linder, D., and Buckel, W. (2000) The involvement of coenzyme A esters in the dehydration of (*R*)-phenyllactate to (*E*)-cinnamate by *Clostridium sporogenes*, *Eur. J. Biochem. 267*, 3874−3884.
22. Tobbell, D. A., Middleton, B. J., Raines, S., Needham, M. R., Taylor, I. W., Beveridge, J. Y., and Abbott, W. M. (2002) Identification of in vitro folding conditions for procathepsin S and cathepsin S using fractional factorial screens, *Protein Expression Purif. 24*, 242−254.
23. Van Duyne, G. D., Standaert, R. F., Karplus, P. A., Schreiber, S. L., and Clardy, J. (1993) Atomic structures of the human immunophilin FKBP-12 complexes with FK506 and rapamycin, *J. Mol. Biol. 229*, 105−124.
24. Otwinowski, Z., and Minor, W. (1997) Processing of X-ray diffraction data collected in oscillation mode, *Methods Enzymol. 276*, 307−326.
25. Terwilliger, T. C., and Berendzen, J. (1999) Automated MAD and MIR structure solution, *Acta Crystallogr., Sect. D 55*, 849−861.
26. Terwilliger, T. C. (2002) Automated structure solution, density modification, and model building, *Acta Crystallogr., Sect. D 58*, 1937−1940.
27. Perrakis, A., Morris, R., and Lamzin, V. S. (1999) Automated protein model building combined with iterative structure refinement, *Nat. Struct. Biol. 6*, 458−463.
28. Leslie, A. G. W. (1992) Recent changes to the MOSFLM package for processing film and image plate data, *CCP4+ESF-EAMCB Newsletter on Protein Crystallography 26*.
29. Jones, T. A., Zou, J. Y., Cowan, S. W., and Kjeldgaard, M. (1991) Improved methods for building protein models in electron-density maps and the location of errors in these models, *Acta Crystallogr., Sect. A 47*, 110−119.
30. Murshudov, G. N., Vagin, A. A., and Dodson, E. J. (1997) Refinement of macromolecular structures by the maximum-likelihood method, *Acta Crystallogr., Sect. D 53*, 240−255.
31. Vagin, A., and Teplyakov, A. (1997) MOLREP: An automated program for molecular replacement, *J. Appl. Crystallogr. 30*, 1022−1025.
32. Guex, N., and Peitsch, M. C. (1997) SWISS-MODEL and the Swiss-PdbViewer: An environment for comparative protein modeling, *Electrophoresis 18*, 2714−2723.
33. Wallace, A. C., Laskowski, R. A., and Thornton, J. M. (1995) LIGPLOT: A program to generate schematic diagrams of protein−ligand interactions, *Protein Eng. 8*, 127−134.
34. Pantoliano, M. W., Petrella, E. C., Kwasnoski, J. D., Lobanov, V. S., Myslik, J., Graf, E., Carver, T., Asel, E., Springer, B. A., Lane, P., and Salemme, F. R. (2001) High-density miniaturized thermal shift assays as a general strategy for drug discovery, *J. Biomol. Screening 6*, 429−440.

BI048481C